Complex Dynamic Models of Star and Delta Connected Multi-phase Asynchronous Motors

Roberto Zanasi
Information Engineering Department
University of Modena e Reggio Emilia
Via Vignolese 905
41100 Modena, Italy
Email: roberto.zanasi@unimore.it

Giovanni Azzone
Information Engineering Department
University of Modena e Reggio Emilia
Via Vignolese 905
41100 Modena, Italy
Email: giovanni.azzone@unimore.it

***Abstract*—This paper addresses the complex modeling of a multi-phase asynchronous motor with star-connected and delta-connected stator phases. The model is obtained using a complex rectangular transformation that reduces the number of complex internal variables and is graphically represented using the Power-Oriented Graphs technique. The dynamic equations have been defined considering the stator phases star-connected and delta-connected, proving that in both cases the internal complex model does not change. Finally some simulation results have been presented to show the effectiveness of the modeled system and the contribution of the star-delta transformation in terms of provided torque.**

I. Introduction

The advantages and the properties of the asynchronous motors in the multi-phase version are well known and described in literature, see for instance [4], together with the ones referred to star-delta connection phases, see [5]. The main focus of this paper is to define a complex reduced dynamic model of a multi-phase asynchronous motor in both star-connected and delta-connected stator phases case and to analyze possible system model differences between the two connection cases. The dynamic equations of the system have been obtained using a "complex" state space transformation and graphically represented using the Power-Oriented Graphs modeling technique. A new transformation that imposes the star or delta connection has been included into the complex model. The paper is organized as follows: Section II presents a brief description of the basic properties of the POG technique in the complex case. In Section III the complex reduced dynamic equations of the considered system are defined and described in the star-connected and delta-connected stator phases cases. Last Section IV shows some simulation results, putting in evidence the differences between the two phases connections in terms of provided torque.

II. Power-Oriented Graphs Technique

The Power-Oriented Graphs technique, see [1] and [2], is suitable for modeling physical systems. The POG is based on the same "energetic ideas" of the Bond Graphs technique, see [3], but it uses a different and specific graphical representation. The POG are normal block diagrams combined with a particular modular structure essentially based on the use of the two blocks shown in Fig. 1.a and Fig. 1.b: the *elaboration block* (e.b.) stores and/or dissipates energy (i.e. springs, masses, dampers, capacities, inductances, resistances, etc.); the *connection block* (c.b.) redistributes the power within the system without storing or dissipating energy (i.e. any type of gear reduction, transformers, etc.). The c.b. transforms the power variables imposing the constraint $\mathbf{x}_1^*\mathbf{y}_1 = \mathbf{x}_2^*\mathbf{y}_2$. The e.b. and the c.b. are suitable for representing both scalar and vectorial systems. In the vectorial case, $\mathbf{G}(s)$ and $\mathbf{K}$ are matrices: $\mathbf{G}(s)$ is always a square matrix of positive real transfer functions; matrix $\mathbf{K}$ can also be rectangular, time varying and function of other state variables. The circle present in the e.b. is a summation element and the black spot represents a minus sign that multiplies the entering variable. The main feature of the Power-Oriented Graphs is to keep a direct correspondence between the dashed sections of the graphs and real power sections of the modeled systems: the real part of the scalar product $\mathbf{x}^*\mathbf{y}$ of the two *power vectors* $\mathbf{x}$ and $\mathbf{y}$ involved in each dashed line of a power-oriented graph, see Fig. 1, has the physical meaning of *the power flowing through that particular section*. Another important aspect of the POG technique is the direct correspondence between the POG representations and the corresponding state space descriptions. For example, the POG scheme shown in Fig. 2 can be represented by the state space equations given in (1) where the *energy matrix* $\mathbf{L}$ is symmetric and positive definite: $\mathbf{L} = \mathbf{L}^* > 0$. When an eigenvalue of matrix $\mathbf{L}$ tends to zero (or to infinity), system (1) degenerates towards a lower

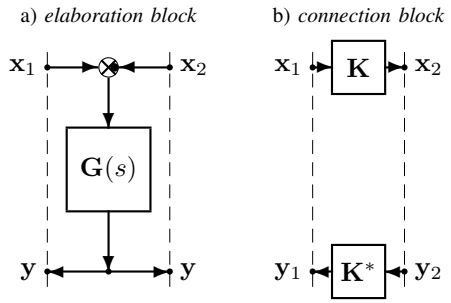

Fig. 1. POG basic blocks: a) *elaboration block*; b) *connection block*.

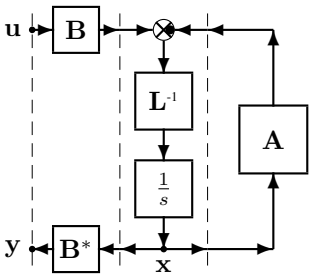

$$\begin{cases} \mathbf{L}\,\dot{\mathbf{x}} = -\mathbf{A}\mathbf{x} + \mathbf{B}\mathbf{u} \\ \mathbf{y} = \mathbf{B}^*\mathbf{x} \end{cases} \quad (1)$$

$$\Downarrow (\mathbf{x} = \mathbf{T}\mathbf{z})$$

$$\begin{cases} \overline{\mathbf{L}}\dot{\mathbf{z}} = -\overline{\mathbf{A}}\mathbf{z} + \overline{\mathbf{B}}\mathbf{u} \\ \mathbf{y} = \overline{\mathbf{B}}^*\mathbf{z} \end{cases} \quad (2)$$

Fig. 2. POG block scheme of a generic dynamic system.

dimension dynamic system. In this case, the dynamic model (2) of the "reduced" system can be directly obtained from (1) by using a simple "congruent" transformation $\mathbf{x} = \mathbf{T}\mathbf{z}$ (matrix $\mathbf{T}$ can also be complex and/or rectangular) where $\overline{\mathbf{L}} = \mathbf{T}^*\mathbf{L}\mathbf{T}$, $\overline{\mathbf{A}} = \mathbf{T}^*\mathbf{A}\mathbf{T}$ and $\overline{\mathbf{B}} = \mathbf{T}^*\mathbf{B}$. If matrix $\mathbf{T}$ is time-varying, an additional term $\mathbf{T}^*\mathbf{L}\dot{\mathbf{T}}\mathbf{z}$ appears in the transformed system. When matrix $\mathbf{T}$ is rectangular, the system is transformed and reduced at the same time. The POG schemes maintain theirs physical meaning even when the dynamic system is described using complex variables.

m_s	: number of stator phases;
m_r	: number of rotor phases;
p	: number of rotor and stator polar expansions;
γ_s	: stator angular phase displacement ($\gamma_s = \frac{2\pi}{m_s}$);
γ_r	: rotor angular phase displacement ($\gamma_r = \frac{2\pi}{m_r}$);
θ_m	: rotor angular position;
ω_m	: rotor angular velocity;
θ_s	: stator voltage angular position;
ω_s	: stator voltage frequency;
θ	: electric angle ($\theta = p\,\theta_m$);
R_s	: stator phases resistance;
L_s	: stator phases self inductance;
M_{s0}	: maximum mutual inductance of the stator phases;
R_r	: rotor phases resistance;
L_r	: rotor phases self inductance;
M_{r0}	: maximum mutual inductance of the rotor phases;
M_{sr0}	: maximum value of the mutual inductance between stator and rotor phases;
J_m	: rotor inertia momentum;
b_m	: rotor linear friction coefficient;
τ_m	: electromotive torque acting on the rotor;
τ_e	: external load torque acting on the rotor.

TABLE I
ELECTRICAL AND MECHANICAL PARAMETERS OF A MULTI-PHASE ASYNCHRONOUS MOTOR.

A. Notations

In this paper the following notations are used to denote full, diagonal, column and row matrices respectively:

$$\underset{1:n}{\overset{i}{[\![}}\, R_{i,j} \,\underset{1:m}{\overset{j}{]\!]}} = \begin{bmatrix} R_{11} & R_{12} & \cdots & R_{1m} \\ R_{21} & R_{22} & \cdots & R_{2m} \\ \vdots & \vdots & \ddots & \vdots \\ R_{n1} & R_{n2} & \cdots & R_{nm} \end{bmatrix}, \qquad \underset{1:n}{\overset{i}{[\![}}\, R_i \,]\!] = \begin{bmatrix} R_1 & & \\ & \ddots & \\ & & R_n \end{bmatrix},$$

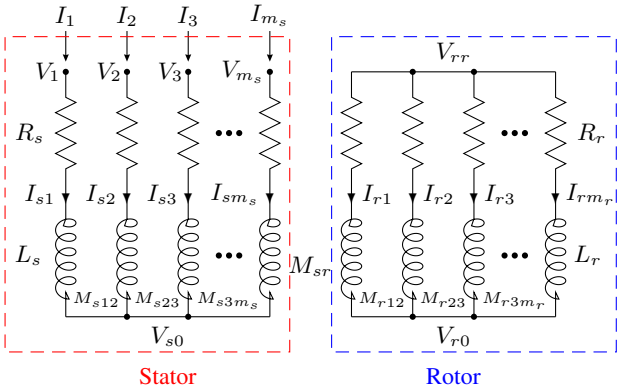

Fig. 3. Electric scheme of a multi-phase asynchronous motor with *star-connected* stator and rotor phases.

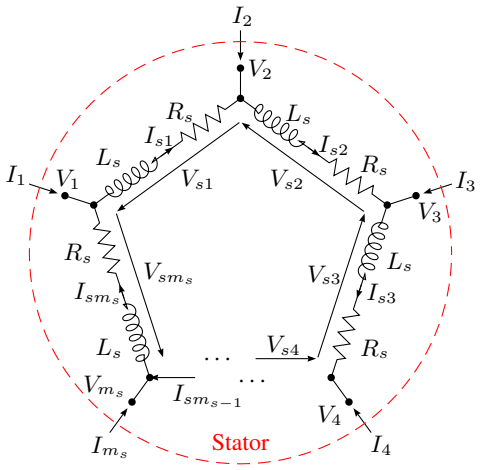

Fig. 4. Electric scheme of stator of the multi-phase asynchronous motor with *delta-connected* phases.

$$\underset{1:n}{\overset{i}{[\![}}\, R_i \,]\!] = \begin{bmatrix} R_1 & R_2 \cdots & R_n \end{bmatrix}^{\mathrm{T}}, \qquad \underset{1:m}{\overset{j}{[\![}}\, R_j \,]\!] = \begin{bmatrix} R_1 & R_2 \cdots & R_m \end{bmatrix}.$$

The symbol $\delta(n)|_k^m$ denote the following function:

$$\delta(n)|_k^m = \begin{cases} 1 & \text{if } n \in [k,\, k \pm m,\, k \pm 2m, \ldots] \\ 0 & \text{in the other cases} \end{cases}$$

where $n, k, m \in \mathbb{Z}$. The symbol $\mathbf{I}_m$ denotes an identity matrix of order m.

III. Electrical Motors Modelling

Let us consider the multi-phase *star-connected* asynchronous motor shown in Fig. 3 with m_s stator phases, m_r rotor phases and characterized by the electrical and mechanical parameters shown in Tab. I. The dynamical behavior of this connection case of the motor will be compared with the behavior of the same motor when the stator phases are *delta-connected* as shown in Fig. 4. Let ${}^t\mathbf{I}_l$ and ${}^t\mathbf{V}_l$ denote the current and voltage *stator-line* vectors:

$${}^t\mathbf{I}_l = \begin{bmatrix} I_1 & I_2 \cdots & I_{m_s} \end{bmatrix}^{\mathrm{T}}, \qquad {}^t\mathbf{V}_l = \begin{bmatrix} V_1 & V_2 \cdots & V_{m_s} \end{bmatrix}^{\mathrm{T}}$$

and let ${}^t\mathbf{I}_s$, ${}^t\mathbf{V}_s$, ${}^t\mathbf{I}_r$ and ${}^t\mathbf{V}_r$ denote the current and voltage *stator-phase* and *rotor-phase* vectors:

$${}^t\mathbf{I}_s = \begin{bmatrix} I_{s1} \; I_{s2} \cdots \; I_{sm_s} \end{bmatrix}^{\mathrm{T}}, \qquad {}^t\mathbf{V}_s = \begin{bmatrix} V_{s1} \; V_{s2} \cdots \; V_{sm_s} \end{bmatrix}^{\mathrm{T}},$$

$${}^t\mathbf{I}_r = \begin{bmatrix} I_{r1} \; I_{r2} \cdots \; I_{rm_r} \end{bmatrix}^{\mathrm{T}}, \qquad {}^t\mathbf{V}_r = \begin{bmatrix} V_{r1} \; V_{r2} \cdots \; V_{rm_r} \end{bmatrix}^{\mathrm{T}}.$$

When the stator phases are *star-connected*, see Fig. 3, the voltage and current *stator-phase* vectors ${}^t\mathbf{V}_s$ and ${}^t\mathbf{I}_s$ are related to the *stator-line* vectors ${}^t\mathbf{V}_l$ and ${}^t\mathbf{I}_l$ as follows:

$${}^t\mathbf{I}_s = {}^t\mathbf{I}_l, \qquad {}^t\mathbf{V}_s = {}^t\mathbf{V}_l - {}^t\mathbf{V}_{s0} \tag{3}$$

where ${}^t\mathbf{V}_{s0} = [1, \; 1, \; \ldots, \; 1]^{\mathrm{T}} V_{s0}$. On the other hand, when the stator phases are *delta-connected*, as shown in Fig. 4, the vectors ${}^t\mathbf{V}_s$, ${}^t\mathbf{I}_s$, ${}^t\mathbf{V}_l$ and ${}^t\mathbf{I}_l$ are related as follows:

$${}^t\mathbf{I}_s = \mathbf{T}_{\vartriangle} \, {}^t\mathbf{I}_l, \qquad {}^t\mathbf{V}_s = \mathbf{T}_{\vartriangle}^{\mathrm{T}} \, {}^t\mathbf{V}_l \tag{4}$$

where matrix $\mathbf{T}_{\vartriangle} \in \mathbb{R}^{m_s \times m_s}$ is structured as:

$$\mathbf{T}_{\vartriangle} = \begin{bmatrix} 1 & 0 & 0 \cdots & -1 \\ -1 & 1 & 0 \cdots & 0 \\ 0 & -1 & 1 \cdots & 0 \\ \vdots & \vdots & \vdots \ddots & \vdots \\ 0 & 0 & 0 \cdots & 1 \end{bmatrix}.$$

Referring to the following state-space vector and input vector respectively:

$$\begin{bmatrix} {}^t\mathbf{I}_s \\ \hline {}^t\mathbf{I}_r \\ \hline \omega_m \end{bmatrix} = \begin{bmatrix} {}^t\mathbf{I}_e \\ \omega_m \end{bmatrix}, \qquad \begin{bmatrix} {}^t\mathbf{V}_l \\ \hline {}^t\mathbf{V}_r \\ \hline -\tau_e \end{bmatrix} = \begin{bmatrix} {}^t\mathbf{V}_e \\ -\tau_e \end{bmatrix}$$

and using the "Lagrangian" approach, as widely described in [6] and [7], the dynamic equations S_t of the multi-phase asynchronous motor expressed with respect to the fixed frame Σ_t are the following:

$$\frac{d}{dt}\left(\left[\begin{array}{c|c} {}^t\mathbf{L}_e & 0 \\ \hline 0 & J_m \end{array} \right] \begin{bmatrix} {}^t\mathbf{I}_e \\ \hline \omega_m \end{bmatrix} \right) = - \left[\begin{array}{c|c} {}^t\mathbf{R}_e + {}^t\mathbf{F}_e & {}^t\mathbf{K}_e \\ \hline -{}^t\mathbf{K}_e^{\mathrm{T}} & b_m \end{array} \right] \begin{bmatrix} {}^t\mathbf{I}_e \\ \hline \omega_m \end{bmatrix} + \begin{bmatrix} {}^t\mathbf{V}_e \\ \hline -\tau_e \end{bmatrix} \tag{5}$$

where matrices ${}^t\mathbf{R}_e$ and ${}^t\mathbf{L}_e$ are defined as follows:

$${}^t\mathbf{R}_e = \begin{bmatrix} {}^t\mathbf{R}_s & 0 \\ 0 & {}^t\mathbf{R}_r \end{bmatrix}, \qquad {}^t\mathbf{L}_e = \begin{bmatrix} {}^t\mathbf{L}_s & {}^t\mathbf{M}_{sr}^{\mathrm{T}} \\ {}^t\mathbf{M}_{sr} & {}^t\mathbf{L}_r \end{bmatrix}$$

where ${}^t\mathbf{R}_s = R_s \mathbf{I}_{m_s}$, ${}^t\mathbf{R}_r = R_r \mathbf{I}_{m_r}$ and the self and mutual inductance matrices ${}^t\mathbf{L}_s$, ${}^t\mathbf{L}_r$ and ${}^t\mathbf{M}_{sr}$ are supposed to assume the following structure:

$${}^t\mathbf{L}_s = L_{s0} \, \mathbf{I}_{m_s} + M_{s0} \left\| \left[\sum_{n=1:2}^{m_s-2} a_n^s \, \cos(n\,(i-j)\gamma_s) \right]_{1:m_s}^{j} \right\|_{1:m_s}^{i},$$

$${}^t\mathbf{L}_r = L_{r0} \, \mathbf{I}_{m_r} + M_{r0} \left\| \left[\sum_{n=1:2}^{m_r-2} a_n^r \, \cos(n\,(i-j)\gamma_r) \right]_{1:m_r}^{j} \right\|_{1:m_r}^{i},$$

$${}^t\mathbf{M}_{sr} = M_{sr0} \left\| \left[\sum_{n=1:2}^{m_{sr}-2} a_n^{sr} \, \cos(n(\theta + i\gamma_r - j\gamma_s)) \right]_{0:m_r-1}^{j} \right\|_{0:m_s-1}^{i}$$

where ${}^t\mathbf{M}_{sr} = {}^t\mathbf{M}_{sr}(\theta)$, $m_{sr} = \min\{m_s, m_r\}$, $L_{s0} = L_s - M_{s0}$ and $L_{r0} = L_r - M_{r0}$. The coefficients a_n^s, a_n^r and a_n^{sr} of the Fourier series satisfy the following constraints:

$$\sum_{n=1:2}^{m_s-2} |a_n^s| \leq 1, \qquad \sum_{n=1:2}^{m_r-2} |a_n^r| \leq 1, \qquad \sum_{n=1:2}^{m_{sr}-2} |a_n^{sr}| \leq 1.$$

Notice that in this way the odd order harmonic injection has been considering, that means that the motor is supposed to have concentrated-windings stator and rotor phases. The torque vector ${}^t\mathbf{K}_e^{\mathrm{T}}$ and matrix ${}^t\mathbf{F}_e$ in (5) are defined as:

$${}^t\mathbf{K}_e^{\mathrm{T}} = \frac{1}{2} \, {}^t\mathbf{I}_e^{\mathrm{T}} \frac{\partial \, {}^t\mathbf{L}_e}{\partial \theta_m}, \qquad {}^t\mathbf{F}_e = -\frac{1}{2} \, {}^t\dot{\mathbf{L}}_e(\theta_m).$$

Let ${}^t\overline{\mathbf{T}}_{\underline{\omega}N} \in \mathbb{C}^{(m_s+m_r+1)\times(m_s+m_r+1)}$ denote the following complex matrix:

$$\begin{aligned} {}^t\overline{\mathbf{T}}_{\underline{\omega}N} &= \begin{bmatrix} {}^t\tilde{\mathbf{T}}_{\underline{\omega}N}(m_s, \theta_s) & 0 \\ 0 & {}^t\tilde{\mathbf{T}}_{\underline{\omega}N}(m_r, \theta_p) \end{bmatrix} \\ &= \underbrace{\begin{bmatrix} {}^t\tilde{\mathbf{T}}_{\underline{\omega}}(m_s, \theta_s) & 0 \\ 0 & {}^t\tilde{\mathbf{T}}_{\underline{\omega}}(m_r, \theta_p) \end{bmatrix}}_{{}^t\overline{\mathbf{T}}_{\underline{\omega}}} \underbrace{\begin{bmatrix} \mathbf{N}_{m_s} & 0 \\ 0 & \mathbf{N}_{m_r} \end{bmatrix}}_{\overline{\mathbf{N}}} \end{aligned}$$

with $\theta_p = \theta_s - \theta$ and matrices ${}^t\tilde{\mathbf{T}}_{\underline{\omega}}(m, \theta) \in \mathbb{C}^{m \times (m+1)/2}$ and $\mathbf{N}_m \in \mathbb{C}^{(m+1)/2 \times (m+1)/2}$ defined as follows:

$${}^t\tilde{\mathbf{T}}_{\underline{\omega}}(m, \theta) = \sqrt{\frac{1}{m}} \begin{bmatrix} \left\| \left[e^{j\,k(\theta - h\gamma_m)} \right] \right\|_{0:m-1}^{1:2:m-2}{}^{k}{}_{h} & \left[\!\left[1 \right]\!\right]_{0:m-1}^{h} \end{bmatrix},$$

$$\mathbf{N}_m = \begin{bmatrix} \sqrt{2}\,\mathbf{I}_{\frac{m-1}{2}} & 0 \\ 0 & 1 \end{bmatrix} \quad \text{where} \quad \gamma_m = \frac{2\pi}{m}.$$

Applying the *pseudo*-transformation ${}^t\mathbf{I}_e = {}^t\overline{\mathbf{T}}_{\underline{\omega}N} \, {}^{\underline{\omega}}\bar{\mathbf{I}}_e$ to system (5), one obtains the following transformed and reduced system $\bar{S}_{\underline{\omega}}$ in the rotating frame $\bar{\Sigma}_{\underline{\omega}}$:

$$\left[\begin{array}{c|c} {}^{\underline{\omega}}\bar{\mathbf{L}}_e & 0 \\ \hline 0 & J_m \end{array} \right] \begin{bmatrix} {}^{\underline{\omega}}\dot{\bar{\mathbf{I}}}_e \\ \hline \dot{\omega}_m \end{bmatrix} = - \left[\begin{array}{c|c} {}^{\underline{\omega}}\bar{\mathbf{R}}_e + {}^{\underline{\omega}}\bar{\mathbf{F}}_e + {}^{\underline{\omega}}\bar{\mathbf{\Omega}}_e & {}^{\underline{\omega}}\bar{\mathbf{K}}_e \\ \hline -{}^{\underline{\omega}}\mathbf{K}_e^* & b_m \end{array} \right] \begin{bmatrix} {}^{\underline{\omega}}\bar{\mathbf{I}}_e \\ \hline \omega_m \end{bmatrix} + \begin{bmatrix} {}^{\underline{\omega}}\bar{\mathbf{V}}_e \\ \hline -\tau_e \end{bmatrix} \tag{7}$$

where ${}^{\underline{\omega}}\bar{\mathbf{R}}_e = {}^t\overline{\mathbf{T}}_{\underline{\omega}}^* \, {}^t\mathbf{R}_e \, {}^t\overline{\mathbf{T}}_{\underline{\omega}} = \mathrm{diag}(R_s \mathbf{I}_{\frac{m_s+1}{2}}, \, R_r \mathbf{I}_{\frac{m_r+1}{2}})$ while matrix ${}^{\underline{\omega}}\bar{\mathbf{L}}_e = {}^t\overline{\mathbf{T}}_{\underline{\omega}}^* \, {}^t\mathbf{L}_e \, {}^t\overline{\mathbf{T}}_{\underline{\omega}}$ is defined as follows:

$${}^{\underline{\omega}}\bar{\mathbf{L}}_e = \left[\begin{array}{cc|cc} \left\| \left[L_{se_k} \right] \right\|_{1:2:m_s-2}^{k} & 0 & \left\| \left[M_{sre_k} \right] \right\|_{1:2:m_s-2}^{l} & 0 \\ 0 & L_{s0} & 0 & 0 \\ \hline \left\| \left[M_{sre_k} \right] \right\|_{1:2:m_r-2}^{k} & 0 & \left\| \left[L_{re_k} \right] \right\|_{1:2:m_r-2}^{l} & 0 \\ 0 & 0 & 0 & L_{r0} \end{array} \right]$$

$$\left[\begin{array}{cc|c} L_{s0}+\frac{m_s}{2}M_{s0}\mathbf{a}_s & M_{sre}\mathbf{a}_{sr}^{\mathrm{T}} & 0 \\ M_{sre}\mathbf{a}_{sr} & L_{r0}+\frac{m_r}{2}M_{r0}\mathbf{a}_r & 0 \\ \hline 0 & 0 & J_m \end{array}\right]\left[\begin{array}{c} {}^{\omega}\dot{\bar{\mathbf{I}}}_s \\ {}^{\omega}\dot{\bar{\mathbf{I}}}_r \\ \hline \dot{\omega}_m \end{array}\right]=-\left[\begin{array}{cc|c} R_s+j\omega_s\mathbf{k}_{m_s}(L_{s0}+\frac{m_s}{2}M_{s0}\mathbf{a}_s) & j\omega_s M_{sre}\mathbf{k}_{m_s}\mathbf{a}_{sr}^{\mathrm{T}} & 0 \\ j\omega_p M_{sre}\mathbf{k}_{m_r}\mathbf{a}_{sr} & R_r+j\omega_p\mathbf{k}_{m_r}(L_{r0}+\frac{m_r}{2}M_{r0}\mathbf{a}_r) & 0 \\ \hline j\frac{p}{2}M_{sre}{}^{\omega}\bar{\mathbf{I}}_r^*\mathbf{k}_{m_r}\mathbf{a}_{sr} & -j\frac{p}{2}M_{sre}{}^{\omega}\bar{\mathbf{I}}_s^*\mathbf{k}_{m_s}\mathbf{a}_{sr}^{\mathrm{T}} & b_m \end{array}\right]\left[\begin{array}{c} {}^{\omega}\bar{\mathbf{I}}_s \\ {}^{\omega}\bar{\mathbf{I}}_r \\ \hline \omega_m \end{array}\right]+\left[\begin{array}{c} {}^{\omega}\bar{\mathbf{V}}_s \\ 0 \\ \hline -\tau_e \end{array}\right] \quad (6)$$

Fig. 5. Complex dynamic equations of a multi-phase asynchronous motor in the transformed frame $\bar{\Sigma}_\omega$.

Moreover, the sum of matrices ${}^{\underline{\omega}}\bar{\mathbf{F}}_e = {}^{t}\overline{\mathbf{T}}^{*}_{\underline{\omega}}\,{}^{t}\mathbf{F}_e\,{}^{t}\overline{\mathbf{T}}_{\underline{\omega}}$ and ${}^{\underline{\omega}}\bar{\mathbf{\Omega}}_e = {}^{t}\dot{\overline{\mathbf{T}}}^{*}_{\underline{\omega}}\,{}^{t}\mathbf{L}_e\,{}^{t}\overline{\mathbf{T}}_{\underline{\omega}}$ in (7) assumes the following structure:

$${}^{\underline{\omega}}\bar{\mathbf{F}}_e + {}^{\underline{\omega}}\bar{\mathbf{\Omega}}_e = \left[\begin{array}{cc|cc} \Big|\Big[j\omega_s k L_{se_k} \Big]\Big|_{1:2:m_s-2}^{k} & 0 & \Big|\Big[j\omega_s k M_{sre_k} \Big]\Big|_{1:2:m_s-2\quad 1:2:m_r-2}^{k\qquad\quad k} & 0 \\ 0 & 0 & 0 & 0 \\ \hline \Big|\Big[j\omega_p k M_{sre_k} \Big]\Big|_{1:2:m_r-2\quad 1:2:m_s-2}^{k\qquad\quad l} & 0 & \Big|\Big[j\omega_p k L_{re_k} \Big]\Big|_{1:2:m_r-2}^{l} & 0 \\ 0 & 0 & 0 & 0 \end{array}\right]$$

where $L_{se_k} = L_{s0}+\frac{m_s}{2}\,M_{s0}\,a_k^s$, $L_{re_k} = L_{r0}+\frac{m_r}{2}\,M_{r0}\,a_k^r$ and $M_{sre_k} = M_{sre}\,a_k^{sr}\,\delta(k)|_l^\infty$. The transformed vectors ${}^{\underline{\omega}}\mathbf{V}_e = {}^{t}\overline{\mathbf{T}}^{*}_{\underline{\omega}N}\,{}^{t}\mathbf{V}_e$ and ${}^{\underline{\omega}}\bar{\mathbf{I}}_e = {}^{t}\overline{\mathbf{T}}^{*}_{\underline{\omega}N}\,{}^{t}\mathbf{I}_e$ have the following structure:

$${}^{\underline{\omega}}\bar{\mathbf{V}}_e = \left[\begin{array}{c} {}^{\underline{\omega}}\bar{\mathbf{V}}_s \\ {}^{\underline{\omega}}\bar{\mathbf{V}}_r \end{array}\right] = \left[\begin{array}{c} {}^{\omega}\bar{\mathbf{V}}_s \\ \hline {}^{\omega}V_{sm_s} \\ \hline 0 \\ 0 \end{array}\right], \quad {}^{\underline{\omega}}\bar{\mathbf{I}}_e = \left[\begin{array}{c} {}^{\underline{\omega}}\bar{\mathbf{I}}_s \\ {}^{\underline{\omega}}\bar{\mathbf{I}}_r \end{array}\right] = \left[\begin{array}{c} {}^{\omega}\bar{\mathbf{I}}_s \\ \hline {}^{\omega}I_{sm_s} \\ \hline {}^{\omega}\bar{\mathbf{I}}_r \\ {}^{\omega}I_{rm_r} \end{array}\right]. \quad (8)$$

Notice that ${}^{\underline{\omega}}\bar{\mathbf{V}}_r = 0$ because the rotor phases are short-circuited. Vectors ${}^{\omega}\bar{\mathbf{V}}_s$, ${}^{\omega}\bar{\mathbf{I}}_s$ and ${}^{\omega}\bar{\mathbf{I}}_r$ are defined as:

$${}^{\omega}\bar{\mathbf{V}}_s = \Big|\Big[{}^{\omega}\bar{V}_{sk} \Big]\Big|_{1:2:m_s-2}^{k} = \Big|\Big[V_{dsk} + j\,V_{qsk} \Big]\Big|_{1:2:m_s-2}^{k},$$

$${}^{\omega}\bar{\mathbf{I}}_s = \Big|\Big[{}^{\omega}\bar{I}_{sk} \Big]\Big|_{1:2:m_s-2}^{k} = \Big|\Big[I_{dsk} + j\,I_{qsk} \Big]\Big|_{1:2:m_s-2}^{k},$$

$${}^{\omega}\bar{\mathbf{I}}_r = \Big|\Big[{}^{\omega}\bar{I}_{rk} \Big]\Big|_{1:2:m_r-2}^{k} = \Big|\Big[I_{drk} + j\,I_{qrk} \Big]\Big|_{1:2:m_r-2}^{k}$$

while the last components ${}^{\omega}V_{sm_s}$, ${}^{\omega}I_{sm_s}$ and ${}^{\omega}I_{rm_r}$ of vectors ${}^{\underline{\omega}}\mathbf{V}_s$, ${}^{\underline{\omega}}\mathbf{I}_s$ and ${}^{\underline{\omega}}\mathbf{I}_r$ in (8) have the following structures:

$${}^{\omega}V_{sm_s} = \sqrt{\tfrac{1}{m_s}}\sum_{h=1}^{m_s} V_{sh} = \sqrt{\tfrac{1}{m_s}}\sum_{h=1}^{m_s}(V_{lh} - V_{s0}),$$

$${}^{\omega}I_{sm_s} = \sqrt{\tfrac{1}{m_s}}\sum_{h=1}^{m_s} I_{sh}, \quad {}^{\omega}I_{rm_r} = \sqrt{\tfrac{1}{m_r}}\sum_{h=1}^{m_r} I_{rh}.$$

The stator and rotor components ${}^{\underline{\omega}}\bar{\mathbf{K}}_s^*$ and ${}^{\underline{\omega}}\bar{\mathbf{K}}_r^*$ of the transformed torque vector ${}^{\underline{\omega}}\bar{\mathbf{K}}_e^* = {}^{t}\bar{\mathbf{K}}_e^*\,{}^{t}\overline{\mathbf{T}}_{\underline{\omega}N} = \left[{}^{\underline{\omega}}\bar{\mathbf{K}}_s^*\ {}^{\underline{\omega}}\bar{\mathbf{K}}_r^*\right]$ assume the following structures:

$${}^{\underline{\omega}}\bar{\mathbf{K}}_s^* = -j\,\frac{p}{2}\left[\begin{array}{c|c} {}^{\omega}\bar{\mathbf{I}}_r^* \Big|\Big[M_{sre_k} \Big]\Big|_{1:2:m_r-2}^{k\qquad\quad l} & {}^{\omega}I_{rm_r} \end{array}\right],$$

$${}^{\underline{\omega}}\bar{\mathbf{K}}_r^* = \quad j\,\frac{p}{2}\left[\begin{array}{c|c} {}^{\omega}\bar{\mathbf{I}}_s^* \Big|\Big[M_{sre_k} \Big]\Big|_{1:2:m_s-2}^{k\qquad\quad l} & {}^{\omega}I_{sm_s} \end{array}\right].$$

Finally, the mechanical torque τ_m can be expressed as follows:

$$\tau_m = \mathrm{Re}\left({}^{\underline{\omega}}\bar{\mathbf{K}}_e^*\,{}^{\underline{\omega}}\bar{\mathbf{I}}_e\right) = \mathrm{Re}\left(\left[{}^{\underline{\omega}}\bar{\mathbf{K}}_s^*\,{}^{\underline{\omega}}\bar{\mathbf{K}}_r^*\right]\left[\begin{array}{c} {}^{\omega}\bar{\mathbf{I}}_s \\ \hline {}^{\omega}I_{sm_s} \\ \hline {}^{\omega}\bar{\mathbf{I}}_r \\ {}^{\omega}I_{rm_r} \end{array}\right]\right)$$

$$= p\,M_{sre}\sum_{k=1:2}^{m_{sr}-2} k a_k^{sr}(I_{drk}I_{qsk} - I_{dsk}I_{qrk}). \quad (9)$$

Let us now consider the last stator equation of system (7) that is represented by the following differential equation:

$$L_{s0}\,{}^{\omega}\dot{I}_{sm_s} = -R_s\,{}^{\omega}I_{sm_s} + {}^{\omega}\,V_{sm_s} \quad (10)$$

When the stator phases are considered *star-connected*, the following relation holds:

$${}^{\omega}I_{sm_s} = \sqrt{\tfrac{1}{m_s}}\sum_{h=1}^{m_s} I_{sh} = 0 \quad (11)$$

Imposing condition (11), equation (10) reduces to:

$${}^{\omega}V_{sm_s} = \sqrt{\tfrac{1}{m_s}}\sum_{h=1}^{m_s}(V_{lh} - V_{s0}) = 0$$

and the expression of the center-star-voltage is given:

$$V_{s0} = \frac{1}{m_s}\sum_{h=1}^{m_s} V_{lh}$$

Whereas, if the stator phases are considered *delta-connected*, the following relation holds:

$${}^{\omega}V_{sm_s} = \sqrt{\tfrac{1}{m_s}}\sum_{h=1}^{m_s} V_{sh} = 0 \quad (12)$$

Substituting (12) in (10), the following differential equation is obtained:

$$L_{s0}\,{}^{\omega}\dot{I}_{sm_s} + R_s\,{}^{\omega}I_{sm_s} = 0 \quad (13)$$

Remark. Equation (13) is a stable dynamic that tends to zero and does not produce any solicitation to the provided torque: one can then remove the last stator equation from (7). Considering that the rotor phases are star-connected

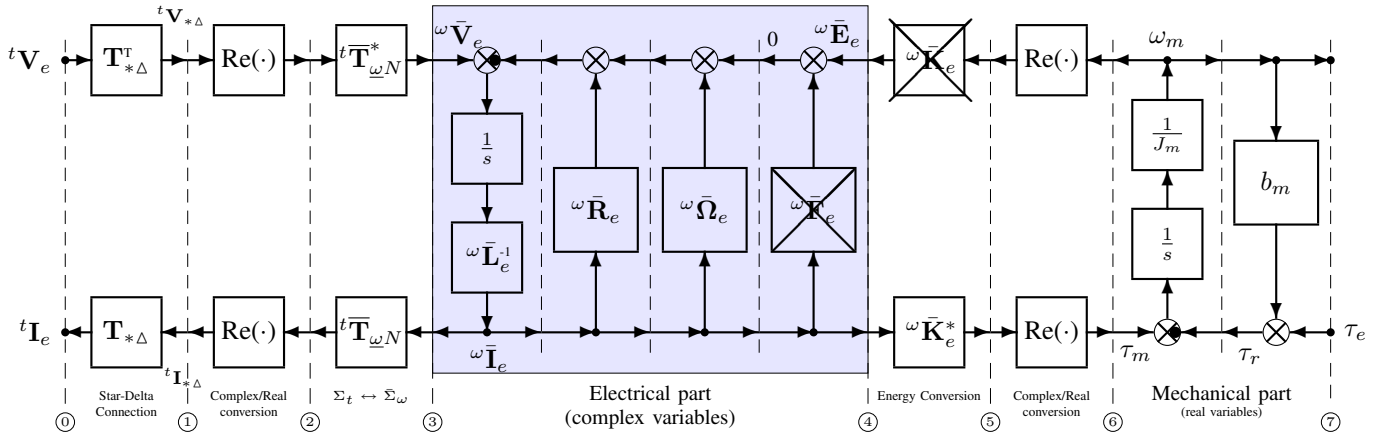

Fig. 6. POG graphical representation of a multi-phase asynchronous motor in the transformed rotating frame $\bar{\Sigma}_\omega$.

and short-circuited, the relations ${}^tV_{ri} = {}^tV_{rr} - {}^tV_{r0} = 0$ and $\sum_{h=1}^{m_r} I_{rh} = 0$ hold: the last rotor equation from (7) can then be removed as well. The resulting reduced dynamic system has now $(m_s + m_r - 2)/2$ complex internal variables instead of $(m_s + m_r + 2)/2$. This demonstrates how the star or delta connection of the stator phases does not change the internal model of the machine.

The resulting reduced system $\bar{S}_\omega$ in the rotating frame $\bar{\Sigma}_\omega$ has the following structure:

$$\left[\begin{array}{c|c} {}^\omega\bar{\mathbf{L}}_e & 0 \\ \hline 0 & J_m \end{array}\right]\left[\begin{array}{c} {}^\omega\dot{\bar{\mathbf{I}}}_e \\ \hline \dot{\omega}_m \end{array}\right] = -\left[\begin{array}{c|c} {}^\omega\bar{\mathbf{R}}_e + {}^\omega\bar{\mathbf{F}}_e + {}^\omega\bar{\mathbf{\Omega}}_e & {}^\omega\bar{\mathbf{K}}_e \\ \hline -{}^\omega\bar{\mathbf{K}}_e^* & b_m \end{array}\right]\left[\begin{array}{c} {}^\omega\bar{\mathbf{I}}_e \\ \hline \omega_m \end{array}\right] + \left[\begin{array}{c} {}^\omega\bar{\mathbf{V}}_e \\ \hline -\tau_e \end{array}\right] \tag{14}$$

whose expanded form is shown in Fig. 5, where $M_{sre} = (M_{sr0}\sqrt{m_s m_r})/2$, $\omega_p = \omega_s - \omega$, $\mathbf{k}_m = \overset{k}{[\![}\, k \,]\!]_{1:2:m-2}$ and where $\mathbf{a}_s$, $\mathbf{a}_r$ and $\mathbf{a}_{sr}$ are real constant matrices defined as follows:

$$\mathbf{a}_s = \left|\!\left[\begin{array}{c} a_k^s \\ \hline \end{array} \right]\!\right|_{1:2:m_s-2}^{k}, \quad \mathbf{a}_r = \left|\!\left[\begin{array}{c} a_k^r \\ \hline \end{array} \right]\!\right|_{1:2:m_r-2}^{k}, \quad \mathbf{a}_{sr} = \left|\!\left[\begin{array}{c|c} a_k^{sr} & \delta(k)|_l^\infty \\ \hline \end{array} \right]\!\right|_{1:2:m_r-2 \;\; 1:2:m_s-2}^{l}.$$

Notice that this system describes the dynamics of the system in both the star-connection case and the delta-connection one. A POG graphical representation of system (14) is shown in Fig. 6. Section ⓪-① represents the *star-delta* transformation matrix $\mathbf{T}_{*\Delta}$ that can assume the following two expressions referred to star or delta connection case respectively:

$$\mathbf{T}_{*\Delta} = \left[\begin{array}{c|c} \mathbf{I}_{m_s} & 0 \\ \hline 0 & \mathbf{I}_{m_r} \end{array}\right], \quad \mathbf{T}_{*\Delta} = \left[\begin{array}{c|c} \mathbf{T}_\Delta & 0 \\ \hline 0 & \mathbf{I}_{m_r} \end{array}\right]$$

and where ${}^t\mathbf{I}_{*\Delta}^{\mathrm{T}} = [\,{}^t\mathbf{I}_s^{\mathrm{T}},\ {}^t\mathbf{I}_r^{\mathrm{T}}]$ and ${}^t\mathbf{V}_{*\Delta}^{\mathrm{T}} = [\,{}^t\mathbf{V}_s^{\mathrm{T}},\ {}^t\mathbf{V}_r^{\mathrm{T}}]$. Section ①-③ represents the real-complex state space transformation $\Sigma_t \leftrightarrow \bar{\Sigma}_\omega$, where function "Re(·)" denotes the "complex to real conversion" of the input. Section ③-④ represents the *Electrical part* of the system that, in this case, is described only by complex matrices and complex variables (the lightly shaded section of Fig. 6). The *Mechanical part* of the motor is described by section ⑥-⑦ which is characterized only by real values and real variables. Section ④-⑥ represents the energy and power conversion (without accumulation nor dissipation) between the electrical and mechanical domains.

Electrical parameters	
$m_s = 5$	$m_r = 5$
$p = 1$	$L_s = 0.17$ mH
$M_{s0} = 0.14$ mH	$R_s = 3\,\Omega$
$L_r = 0.15$ mH	$M_{r0} = 0.13$ mH
$R_r = 2\,\Omega$	$M_{sr0} = 0.12$ mH
$V_{max} = 100$ V	$\omega_s = 8\pi$ rad/s
Mechanical parameters	
$J_m = 0.75$ Kg m^2	$b_m = 0.45$ Nm s/rad
$\tau_e = 2$ Nm	

TABLE II
ELECTRICAL AN MECHANICAL PARAMETERS OF THE SIMULATED MOTOR MODEL.

IV. SIMULATION RESULTS

The model of the multi-phase asynchronous motor represented in Fig. 6, whose equations are described in Fig. 5, has been implemented in Matlab/Simulink. The simulation results presented in this section have been obtained using the electrical and mechanical parameters listed in Tab. II. The input balanced stator voltage vector that has been considered is:

$${}^t\mathbf{V}_l = \overset{h}{[\![}\, V_{lh} \,]\!]_{1:5} = \sum_{k=1:2}^{3} \overset{h}{[\![}\, V_{mk} \cos(k\,(\theta_s - (h-1)\gamma_s)) \,]\!]_{1:5} \tag{15}$$

where k indicates the injected harmonic order. Let us consider $\mathbf{a}_s = \mathbf{a}_r = \mathbf{a}_{sr} = diag\,[\,0.7 \quad 0.3\,]$ as self and mutual inductances coefficient matrices. The method adopted to define the V_{mk} voltages of (15), has been to choose the fundamental voltage amplitude V_{m1} and then scaling V_{m3} using a percentage coefficient $K_1^3 = V_{m3}/V_{m1} = V_{ds3}/V_{ds1} = 15\%$, that indicates the percentage of 3^{rd} harmonic component amplitude with respect to the fundamental. In Fig. 7(a) the time behavior of the stator voltage vector ${}^t\mathbf{V}_s$, the stator current vector ${}^t\mathbf{I}_s$ and the rotor current vector ${}^t\mathbf{I}_r$ in the range $t \in [0, 2]$ s is shown considering the stator phases star-connected, while in Fig. 7(b) it is shown the same vectors evolution but in the delta-connection case: notice that the delta-connection is characterized by a higher current absorption compared with

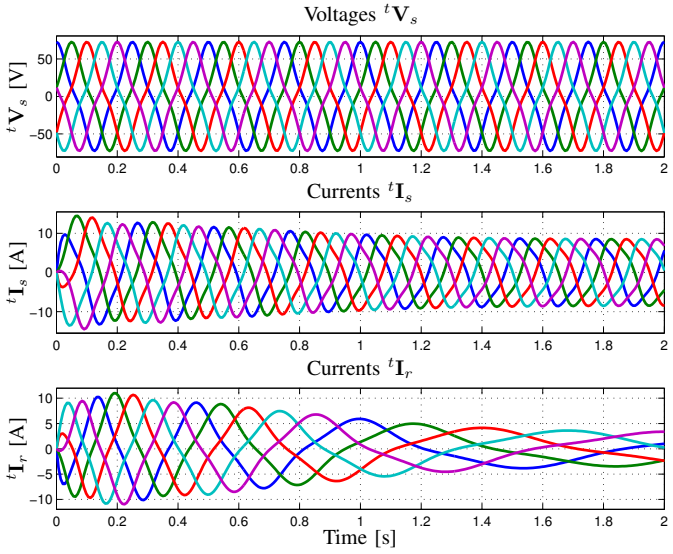

(a) Star-connection

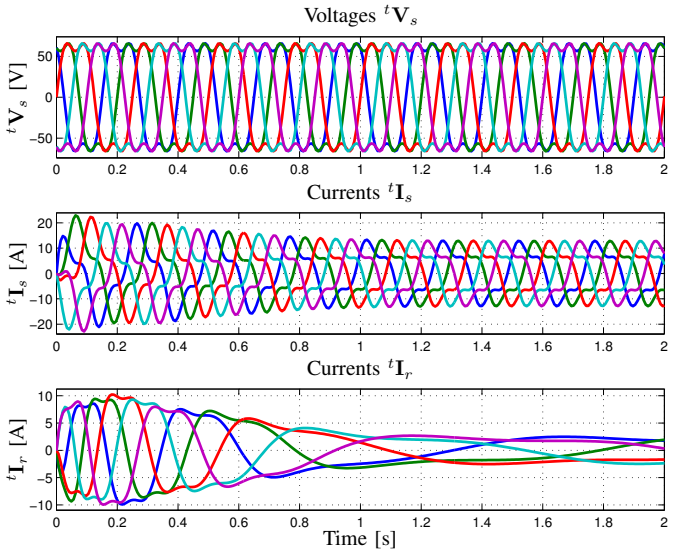

(b) Delta-connection

Fig. 7. Star-connected and delta-connected stator phases: stator voltage vector ${}^t\mathbf{V}_s$, stator current vector ${}^t\mathbf{I}_s$ and rotor current vector ${}^t\mathbf{I}_r$ in the original reference frame Σ_t.

the star-connection. This aspect explains how the dynamic mechanical torque increases when the stator phases are delta-connected (Fig. 8(a) and Fig. 8(b)), even if τ_m has the same expression (9) in both stator phases connection cases. In Fig. 8(a) the mechanical torque τ_m is shown as function of the time in the range $t \in [0, 2]$ s and in Fig. 8(b) as function of the angular velocity in the range $\omega_m \in [0, 22.5]$ rad/s, with star-connected stator phases (blue plots) and delta-connected stator phases (red plots).

V. Conclusions

In the paper a general complex dynamic model of a multi-phase asynchronous motor with star-connected and delta-connected stator phases has been obtained and graphically

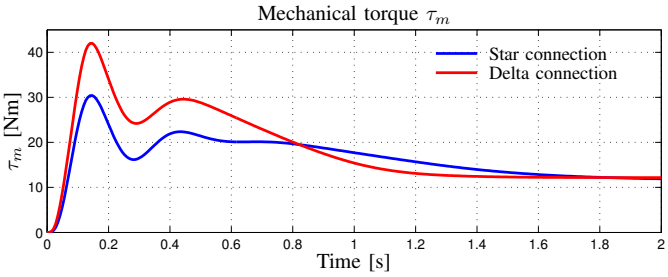

(a) Mechanical torque VS Time

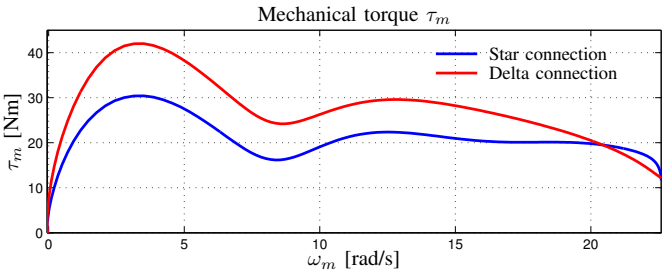

(b) Mechanical torque VS Angular velocity

Fig. 8. Mechanical torque τ_m with star-connected and delta-connected stator phases as function of the time (a) and as function of the angular velocity (b).

represented using the POG technique. A complex transformation has been used in order to reduce the number of the complex internal variables and a new transformation matrix that imposes the star or delta connection of the stator phases has been defined and included in the model. It has been demonstrated that the star/delta transformation does not change the internal complex equations model of the motor. The model has then been implemented in Matlab/Simulink and the simulation results have shown and compared the star and delta connection cases.

References

[1] R. Zanasi, *Power Oriented Modelling of Dynamical System for Simulation*, IMACS Symp. on Modelling and Control, Lille, France, May 1991.

[2] R. Zanasi, *The Power-Oriented Graphs Technique: system modeling and basic properties*, 6th IEEE VPPC, Lille, France, Sept. 2010.

[3] D. C. Karnopp, D.L. Margolis, R. C. Rosemberg, *System dynamics - Modeling and Simulation of Mechatronic Systems*, Wiley Interscience, ISBN 0-471-33301-8, 3rd ed. 2000.

[4] E. Levi, R. Bojoi, F. Profumo, H.A. Toliyat, S. Williamson, *Multiphase induction motor drives - A technology status review*, IET Electr. Power Appl., vol. 1, no. 4, pp. 489-516, July 2007.

[5] P. Pillaya, R.G. Harleya, E.J. Odendala, *A Comparison Between Star and Delta Connected Induction Motors When Supplied by Current Source Inverters*, Electric Power Systems Res., vol. 8, no. 1, pp. 41-51, April 1984.

[6] R. Zanasi, F. Grossi, G. Azzone, *The POG technique for Modeling Multi-phase Asynchronous Motors*, 5th IEEE International Conference on Mechatronics, Málaga, Spain, 14-17 April 2009.

[7] R. Zanasi, G. Azzone, *Complex Dynamic Model of a Multi-phase Asynchronous Motor*, ICEM - International Conference on Eletrical Machines, Rome, Italy, 6-8 Sept. 2010.

[8] G. Azzone, *Modeling and Control of Multi-phase Asynchronous Electrical Motors*, PhD Thesis, Feb. 2011.